International Institute for
Applied Systems Analysis
www.iiasa.ac.at

Modeling Electricity Production-Demand Correlations for STEC Plants in Dispersed Locations

Balabanov, T.

IIASA Working Paper

WP-81-159

December 1981

MODELING ELECTRICITY PRODUCTION-
DEMAND CORRELATIONS FOR STEC PLANTS
IN DISPERSED LOCATIONS

Todor Balabanov

December 1981
WP-81-159

PREFACE

It has been a recent task of IIASA's Energy Systems Program to study solar energy and in particular opportunities for deploying large-scale solar technologies for electricity production in a set of countries.

In this context the present simulation model was developed. This model called STECP was used to investigate the electrical output of solar plants with and without internal thermal storage that were conceived to be spread across three different time zones.

As a result, it appears that a higher reliability of electricity supply can be achieved if the solar plants are sited in dispersed locations than if they were concentrated in one place. Introduction of internal thermal storage in the system of solar plants increases its seasonal electric output from two to three times and decreases external storage requirements.

The model, which is described here along with some application results, permits a consistent investigation of the electricity production-demand correlation for a system of solar electric plants.

CONTENTS

1. INTRODUCTION

It has been one of the recent tasks of IIASA's Energy Systems Program to study solar energy and, in particular, opportunities for the deployment of large-scale solar technologies for electricity production in different countries. The core assumption of this study is that the electricity produced by solar plants in the South of Europe is used to meet the electricity demands of the producing countries as well as of a set of other European countries.

It is the idea of solar plants sited in dispersed locations that has invoked the present study. Main points of interest are the following:

-- What are the realistic parameters (reliability of supply, mirror area, etc.) for a STEC plant under site-specific conditions?
-- How do diverse local climates affect the overall, integrated output of the plants situated in different countries?
-- What is the influence of internal thermal storage introduced in the system of STEC plants on the system's electricity supply potential?

A simulation model named STECP (Solar Thermal Electricity Conversion Performance) was built by the author to explore these questions. The model is described in Section 3. Furthermore, it has been used to evaluate on a yearly basis the performance characteristics of two types of STEC plants assumed to be set up in 7 Southern European countries. The underlying approach is

presented in Section 2, and the actual assumptions and numerical results are given in Sections 4 and 5.

2. APPROACH USED

STECP is developed to characterize the hourly electrical output of solar plants with a central tower and field of heliostats. Direct beam solar radiation data are obtained and scaled for use in the seven sample southern countries. For each of those countries the land potentially available for solar electricity production is evaluated as a function of the annual average solar radiation level. It is split into three zones according to radiation levels.

Consideration centers on two types of STEC plants: STEC 1 without built-in thermal storage and STEC 2 with 12 hours of thermal storage. Their deployment on the land potentially available is designed in such a way that the installed capacities meet the power requirements of the producing countries in the South as well as of other European countries for a given year (1979) (see Section 4 for details).

In order to investigate the electricity production-demand correlation on an hour-per-hour basis three deployment cases are considered:

Case 1. STEC 1 plants without storage located at one point;
Case 2. STEC 1 plants without storage set up in the seven producing countries;
Case 3. Combination of plants with and without storage set up in the seven countries, two-thirds of the land available is devoted to STEC 1 without storage, and one-third to STEC 2 with 12 hours storage; STEC 2 plants are conceived to work in the load following mode.

The same overall installed capacity is assumed for all those cases. Numerous model runs are made for four seasons of the year and the three cases in order to

-- evaluate the required area of mirrors and volume of internal storage as a function of capacity factor and radiation zone;
-- determine the average solar shares per season in the total electricity production;
-- compare the cases in terms of total installed capacity and volume of external storage to be introduced if all the electricity demands had to be met fully (100%) by solar electricity.

3. THE SOLAR THERMAL ELECTRIC CONVERSION PERFORMANCE (STECP) MODEL

3.1. System Description and Assumptions

In order to model solar electricity production, one has to formalize the behavior of the main components of a STEC plant as described below, subject to stochastic solar radiation inputs (E(t), Figure 1), as well as their operational algorithm. This has been done under consideration of an exogenously given daily electricity demand profile $P_e^d(t)$. The main system components, schematized in Figure 1 and discussed in this section, are the following.

-- The field of the heliostats, which accepts and concentrates solar radiation onto the absorber-boiler;

-- The absorber-boiler, which transforms optical energy into heat energy of the working fluid; this module also includes the associated piping to and from the turbine and/or to the thermal storage.

-- The dispatcher-controller, which controls the operational algorithm of the plant;

-- The turbogenerator set, which consists of a steam turbine with two steam inlets and a generator with a rated power of 100 MW;

-- Thermal storage, which consists of approximately 18,500 cast iron blocks 6 tons each, linked as parallel heat exchangers on the input and output sides. This system capacity is conceived to back 12 hours of load equal to the rated generator power of 100 MW, upon prior heating of the storage material to 600°C by the inlet steam.

3.1.1. Assumptions

The performance of a solar thermal power plant with a central tower surrounded by a field of heliostats depends on the level of direct beam insolation, allocation pattern of the heliostats in the field, precision of heliostat acceptance and reflection, design characteristics of the receiver-absorber including thermal losses, losses of the transport system, efficiencies of the heat exchanger and turbine generator set, characteristics of the thermal storage system, and the operational algorithm of the plant. In order to simulate hourly performance over an entire year, several assumptions have been introduced including:

-- Optimal allocation of the heliostats in the field (minimal shadowing and blocking losses);

-- Uniform distribution of solar radiation over the heliostat and receiver surface;

-- Steady-state operation of the equipment;

-- Constant input/output temperatures of the receiver-absorber;

-- Constant optical characteristics of the reflecting and absorbing surfaces;
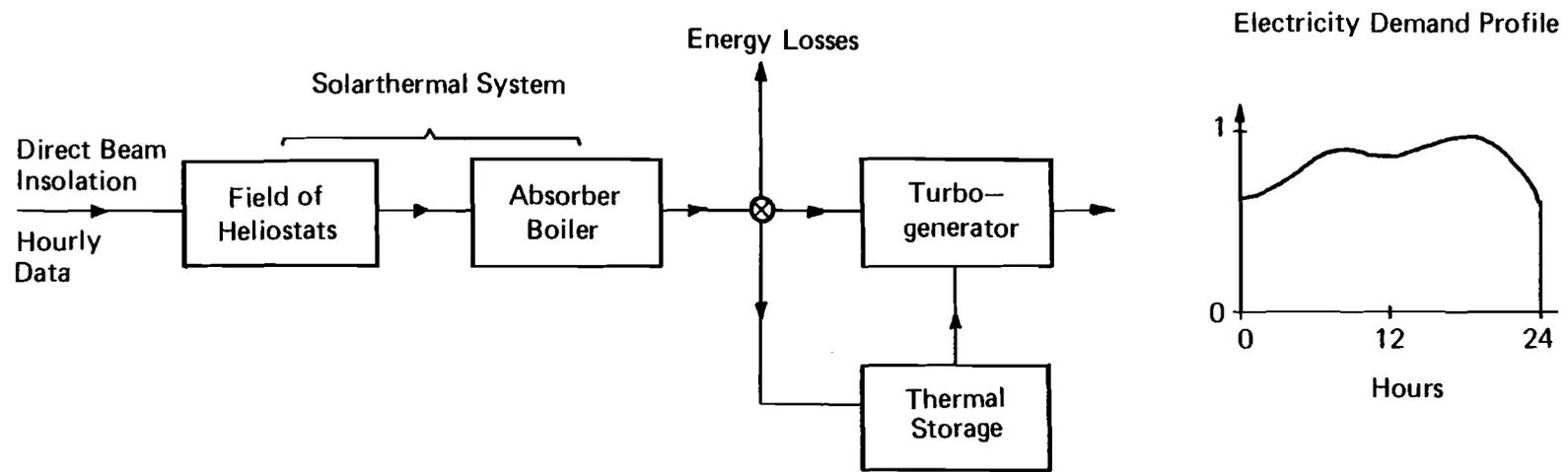
Figure 1. Main components and exogenous variables of the system.

-- Two temperature and pressure levels for the steam flow in the turbine, namely level 1 from the receiver absorber and level 2 from the thermal storage;

-- Piping, transport, and startup losses are accounted for through the receiver-absorber efficiency, etc.

Based on these assumptions, it is felt that the overall error in evaluation of the system's characteristics is not more than 10%.

3.2. Solar Angles Geometry Used in the Model

Three solar angles have been used to characterize the sun's position (see, e.g., Fujita et al. 1978, Duffie 1974):

λ latitude (north, positive);

δ declination (i.e., the angular position of the sun at solar noon with respect to the plane of the equators; north, positive);

τ hour angle (i.e., solar noon being zero, and each hour equaling 15° of longitude with mornings positive and afternoons negative).

The declination angle can be obtained from Cooper's approximation (1969):

$$\delta = 23.45 \cdot \sin [360 \, \frac{284+n}{365}], \qquad [°] \qquad (1)$$

where n is the day of the year.

The hour angle is given by

$$\tau = 15 \, (i-12), \qquad [°] \qquad (2)$$

where i is the hour of the day.

Given Equations (1) and (2) one obtains θ_s, the angle determining the sun's position relative to the vertical of the field, as shown in Figure 2:

$$\cos \theta_s = \sin \lambda * \sin \delta + \cos \lambda * \cos \delta \cdot \cos \tau, \qquad [°] \qquad (3)$$
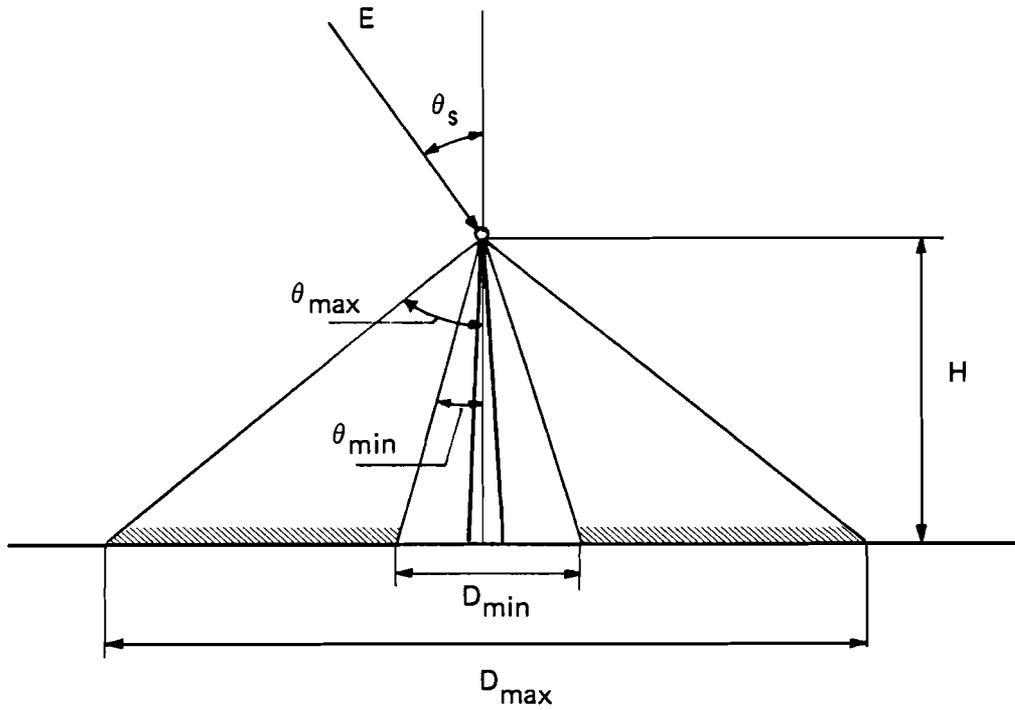
E	Intensity of direct beam insolation (kcal/m^2/h)
θ_s	Sun's position, relative to field vertical (^{o})
$\theta_{max, min}$	outer, inner field angle (^{o})
$D_{max, min}$	outer, inner field diameter (m)
H	Tower height (m)

Figure 2.   Representation of the field of heliostats and the sun's position in the model.

3.3. Modeling the Field of Heliostats

Let us first define the terms to be used (see also Figure 2): A_m, the total mirror area, is given as

$$A_m = \pi \cdot H^2 \, (tg^2\theta_{max} - tg^2\theta_{min}) \quad , \tag{4}$$

where

H = tower height [m];
θ_{max} = outer angle of the field [$^{\circ}$];
θ_{min} = inner angle of the field [$^{\circ}$];

In accordance with Riaz (1976) and Balabanov (1981) the active area of the heliostats (A_o) of the field visible simultaneously from the sun and the absorber-receiver (Figure 2) could be described as a function of the angular position of the sun over the field.

for $\Theta_s \leq \Theta_{min}$,

$$A_o = 2\Pi \cdot H^2 \int_{\Theta_{min}}^{\Theta_{max}} \sin\Theta_f * \frac{1}{\cos^2\Theta_f} \, d\Theta_f = 2\Pi \cdot H^2 \left(\frac{1}{\cos\Theta_{max}} - \frac{1}{\cos\Theta_{min}} \right) ; \tag{5}$$

for $\Theta_{min} \leq \Theta_s$,

$$A_o = 2\Pi \cdot H^2 \left[\int_{\Theta_{min}}^{\Theta_{max}} \sin\Theta_f * \frac{1}{\cos^3\Theta_f} * \cos\Theta_s * d\Theta_f + \int_{\Theta_{min}}^{\Theta_{max}} \sin\Theta_f * \frac{1}{\cos\Theta_f} \, d\Theta_f \right]$$

$$= \cdot H^2 \left(2 \, \frac{1}{\cos\Theta_{max}} - \cos\Theta_{min} * \frac{1}{\cos\Theta_{min}} - \frac{1}{\cos\Theta_s} \right) ; \tag{6}$$

for $\Theta_s \geq \Theta_{max}$,

$$A_o = 2 \cdot \Pi H^2 \int_{\Theta_{min}}^{\Theta_{max}} \sin\Theta_f * \frac{1}{\cos^3\Theta_f} * \cos\Theta_f * d\Theta_f$$

$$= \Pi \cdot H^2 (tg^2\Theta_{max} - tg^2\Theta_{min}) * \cos\Theta_s . \tag{7}$$

The share of the active area in the total area, $\eta=A_o/A_m$, could be computed from

for $\theta_s \leq \theta_{min}$,

$$\eta = 2*(arcos\theta_{max}+arcos\theta_{min})^{-1} \; ; \tag{8a}$$

for $\theta_{min}<\theta_s<\theta_{max}$,

$$\eta = \frac{2*arcos\theta_{max}-cos\theta_s*arcos^2\theta_{min}-arcos\theta_s}{arcos^2\theta_{max}-arcos^2\theta_{min}} \; ; \tag{8b}$$

for $\theta_s \geq \theta_{max}$,

$$\eta = cos\,\theta_s \; . \tag{8c}$$

Equation (8), representing the active area of the field as a function of the sun's position ($\eta=f(\theta_s)$), serves as a basis for computing the heat production of the field of heliostats, $Q_f(t)$ [kWh/h]. In accordance with the assumptions stated in Section 3.1., the other field performance indicators are constant with an estimated value of $\eta_2=0.861$, which takes into account the uncertainties of the assumptions (Balabanov 1981, Fujita et al. 1978).

3.4. Receiver-Absorber Performance

In accordance with Balabanov (1981), the receiver-absorber performance for a steady-state operational condition could be computed as:

$$Q_r(t) = \eta_{ra}Q_f(t) - U_x(T_x-T_A) \; , \tag{9}$$

where

$Q_r(t)$ = output from the receiver [kWh/h];

$Q_f(t)$ = heat production of the field [kWh/h] of heliostats;

η_{ra} = performance indicator of the receiver absorber and associated piping; value η_{ra} = 0.91 was assumed (Balabanov 1981);

U_x = thermal conductivity of boiler insulation;

T_x = average temperature of working fluid;

T_A = ambient temperature;

$U_x(T_x-T_A)$ = thermal losses in the ambient atmosphere [kWh/h].

Because of the lack of data for the ambient temperature for most of the places considered it is assumed after Balabanov (1981) that

$$U_x(T_x - T_A) = 0.03 \, Q_f(t) \quad .$$

Hence Equation (9) takes the following form

$$Q_r(t) = (\eta_{ra} - 0.03) \, Q_f(t) \quad . \qquad\qquad \text{[kWh/h]} \qquad (10)$$

3.5. Modeling Thermal Storage

The behavior of the modular storage with a parallel input link operating with sensible heat that is added to the storage medium is described as in Balabanov (1981) by

$$\sum_{j=1}^{m} M_j C_j \, \frac{dT(t)}{dt} + k(T_j(t) - T_o(t)) = \Delta Q(t) \quad , \qquad (11)$$

where

$\Delta Q(t)$ = heat energy contained in the storage [kWh];

$j = 1, \ldots m$ = number of components of the heterogenous storage material;

M_j = weighted average mass of the component j of the storage [10^3 kg];

k = number of zones with a weighted temperature;

C_j = specific heat capacity of the component j of the storage material [$\frac{kWh}{^oC \cdot kg}$];

$T_o(t)$ = weighted ambient temperature around the storage (^{o}C);

$T_j(t)$ = weighted temperature of the component j of the storage material (^{o}C).

For the computer implementation, Equation (11) is put into the discrete form

$$\sum_{j=1}^{m} M_j C_j \, \frac{dT(t)}{dt} = Q_{st}^r(t) - Q_{st}^t(t) - k(T_j(t) - T_o(t)) \quad , \quad (12)$$

where

$Q_{st}^r(t)$ = heat flow into storage from receiver (kWh);

$Q_{st}^t(t)$ = flow extracted from storage into turbine generator set (kWh).

The component $k(T_j(t) - T_o(t))$ represents thermal losses to the environment. The component $\sum_{j=1}^{m} M_j C_j$ jointly with the lower and upper temperature levels determines the thermal capacity of the storage.

In the present case, thermal capacity is measured in hours necessary for full load of the plant to be covered with the heat extracted from the storage. The indicators of storage charge are maximum and minimum temperatures of the storage media, i.e., 600^oC and 300^oC, respectively.

3.6. Modeling the Turbine-Generator Set

The set consists of a turbine, condenser, regenerative heaters, pumps, and a generator with a rated power of 100 MW. The efficiencies of various optimized Rankine cycle configurations have been correlated as a function of power output, cycle temperatures and pressures, and generic class according to Sandia Laboratories, Albuquerque (Fujita et al. 1978). For present purposes different inlet temperatures of the steam turbine have been assumed; one inlet directly coupled to the receiver absorber is at 560°C (p=70 bar), and the other accepting storage-derived vapor is at 430°C (p=70 bar). The condensing temperature is assumed to be 40°C, and regenerative heaters are assumed to raise the inlet boiler fluid temperature to 260°C. Under these conditions, the overall turbine cycle efficiency η_T (from the heat in the steam to electricity) is given by the empirical formulae

for the 560°C inlet,

$$\eta_T = 0.159 + 0.0658 \log (P_e^{max}) = 0.00517 \cdot [\log(P_e^{max})]^z \quad ; \quad (13)$$

and for the 430°C inlet,

$$\eta_T = 0.134 + 0.0556 \log (P_e^{max}) - 0.00437 \cdot [\log P_e^{max}]^z \quad ; \quad (14)$$

where

P_e^{max} = peak electrical output, kW(e), and

η_T = overall cycle efficiency.

For P_e^{max} = 100,000 kW(e), the overall cycle efficiency is 0.36025 (560°C) and 0.30275 (430°C), respectively.

3.7. Operational Algorithm of a STEC Plant

For the STEC plant described in Figure 1, the following operational algorithm is assumed:

-- If the heat flow from the receiver ($Q_r(t)$) is sufficient for meeting the load demanded ($P_e^d(t)$) it is dispatched to the turbine;
-- If Q_r is smaller than the demand and if the temperature of the storage is above minimum the heat needed to meet the load is taken from the storage.
-- If the storage temperature is below minimum the demands are met only by Q_r;
-- If Q_r is greater than the demand and the storage temperature is below maximum the demand is met, and the additional heat is transferred into the storage;
-- If Q_r is greater than the demand and the storage temperature is above maximum level the heat above the load is rejected (marked as losses in Figure 1).

For plants without thermal storage the component $\sum_{j=1}^{m} M_j C_j$ in Equation (12) is set to zero.

Based on the methodology described, a set of computer programs was developed and used for the case study described below.

4. ASSUMPTIONS FOR THE CASE STUDY

The main idea is to use the land currently not used for other purposes for solar electricity production in countries such as Portugal, Spain, southern France, Italy, Yugoslavia, Greece, and in part of Turkey.

The electricity produced is distributed among the producer countries as well as among most other European countries, in order to meet their hourly electricity demands. In order to integrate those demands the following countries are grouped into three hourly zones (see Budyko 1963):

I   Belgium, France, Luxembourg, Netherlands, Portugal, Spain, and the UK;
II Austria, F.R.G., Italy, and Switzerland;
III Greece, Turkey, and Yugoslavia.

Table 1 shows the locations considered for solar electricity production, the time zone they belong to, their latitude, and the estimated land potential suitable for solar electricity production split into three radiation zones. The estimated land potential is based on a study done by Claire Doblin (IIASA, private communication, 1981).

As can be seen from Table 1, about 60% of the land potential is located in Turkey, far away from the centers of electricity demand. Accordingly, 18% per hourly production of Turkey's electricity production is subtracted as transmission losses, whereas the transmission losses for the other producing countries are assumed to be zero.

4.1. Calibration of Direct Solar Beam Radiation

The initial intention of the team collecting radiation data (Tony Ward and the author) was to obtain hourly records of direct beam radiation for at least one location per country mentioned in Table 1. Inspite of several months of intensive research this plan was found to be inoperable. Only one tape with hourly records for Carpentras in southern France was at hand, and a few atlases with average solar data (see reference list). The tape, however, contained 8 subsequent full years of measurement, and straightforward comparison of the monthly averages (see Table 2) showed a substantial difference between the years, suggesting that the statistical properties of the solar radiation for different years may differ as well (see also Balabanov 1981).

Table 1. Locations considered in the study and their main characteristics.

Locations	Time Zone	Geogr. Latit. [°N]	Land potential [10^3km^2) split into radiation zones					
			I*		II*		III*	
			Total	20% of total	Total	20% of total	Total	20% of total
1. Portugal	(1)	38.43	1.7	0.34	–	–	–	–
2. Spain	(1)	40.27	6.5	1.3	7.2	1.44	0.7	0.14
3. S. France	(1)	44.05	3.5	0.7	–	–	–	–
4. Italy	(2)	38.12	0.8	0.16	1.6	0.32	0.8	0.16
5. Yugoslavia	(2)	41.59	1.8	0.36	0.6	0.12	–	–
6. Greece	(3)	33.5	–	–	0.9	0.18	0.9	0.18
7. Turkey (1/3 share)	(3)	37.6	14.3	2.86	13.1	2.62	13.1	2.62
Total			28.6	5.72	23.4	5.16	15.5	3.1

*In accordance with the level of the normal beam solar radiation [kWh/m^2/day]:
Zone (1) - 4.64; Zone (2) - 5.27; Zone (3) - 5.9.

Table 2. Monthly averages of direct radiation = > joule/cm^2/day* (Carpentras 1971-1978).

	Month	1971	1972	1973	1974	1975	1976	1977	1978
Winter	1	750	750	1013	828	712	1534	626	866
	2	1697	719	1509	1029	1365	847	1102	860
	3	1606	1266	1713	735	1235	1690	1321	1475
Spring	4	1233	1803	1936	1380	1883	1514	2114	1406
	5	1339	1971	1909	1380	1842	2378	1331	1644
	6	2313	1861	2315	2372	2340	2667	1915	2130
Summer	7	2436	2539	2368	2956	2875	2377	2194	2730
	8	2236	2146	2059	2581	2045	2080	2013	2412
	9	1856	1525	2024	1627	1248	1631	2003	2418
Fall	10	1379	1064	1481	1623	1635	1039	1213	1737
	11	1037	727	1206	998	771	1165	1206	1218
	12	927	840	1076	1149	761	765	1023	607
		Lisbon (Central Portugal)	Madrid (Central Spain)	Carpentras (Southern France)	Messina (Southern Italy)	Skopje (Southern Yugoslavia)	Central Turkey	Athens (Greece)	

*1 J/cm^{2}h = 2.39 kcal/m^{2}h = 0.00278 kWh/m^{2}h

On that basis hourly levels of direct beam radiation of
Carpentras were adjusted to the levels of the other locations
considered. The underlying comparison (see also Ward 1982) of
the monthly averages for Carpentras with relevant data sets for
the other six locations led to the factors outlined in Table 3.
This was done by dividing the monthly averages for the other
locations by the respective averages for Carpentras for certain
years (see Table 2).

Table 3. Factors applied to hourly beam radiation for Carpentras
          to generate data for other stations in the south of
          Europe for the selected months (see also Ward 1982).

Location	January	April	July	October
Lisbon	1.19	1.19	1.03	1.30
Madrid	1.20	1.17	0.99	1.12
Messina	1.23	1.02	0.93	1.2
Athens	1.02	1.04	0.93	1.23
Skopje	0.62	0.85	0.78	0.92
Central Turkey	1.28	1.11	1.11	1.63

The months of January, April, July, and October were
selected as representative of the four seasons. In the scaling
process care was taken to avoid exceeding of an hourly maximum
radiation level of 1 kWh/m^2.

In order to account for stochastic differences between the
locations, a representative year (Table 2) was randomly assigned
and the hourly values obtained were adjusted accordingly.

4.2. Demands for Electricity

The daily load profiles of the hourly electricity demands
for all the countries listed in the introduction to Section 4
are based on UCPTE (1979) statistics for representative days of
each of the seasons in 1979. Based on these values, the inte-
grated overall seasonal load profiles of the country were com-
puted after considering the time shifts associated with the
different time zones (e.g., +1 hour for the U.K., -0 for the
F.R.G., and -1 for Turkey). For computational convenience the
hourly load profiles were normalized with respect to the hour
of maximum (100%) load (Table 4). The numerical values given
in the footnote to Table 4 are of the order of 200 GW.

Table 4. Integrated daily load profiles normalized to the daily maximum.

Spring	76.0*	74.0	74.0	73.0	74.0	78.0	83.0	86.0	98.0	99.0	100.0**	98.0
	96.8	96.0	95.3	93.0	92.4	96.0	97.1	95.0	94.1	91.0	88.7	80.0
Summer	70.7*	68.0	64.6	66.0	67.5	75.0	83.0	92.0	98.5	99.0	100.0**	98.0
	96.6	95.0	94.5	92.0	90.2	89.0	86.7	86.5	86.1	84.0	81.8	74.0
Fall	68.7*	65.0	63.5	64.0	65.8	72.0	81.7	90.0	97.6	98.0	100.0**	97.0
	92.5	94.0	95.6	93.0	89.4	89.2	89.2	81.0	92.7	86.0	81.0	70.0
Winter	81.4*	80.0	78.7	77.5	76.9	80.0	83.4	90.0	97.4	99.0	100.0**	99.0
	98.1	97.0	96.9	98.0	99.0	99.0	100.0	98.0	97.0	90.3	86.0	80.0

*12.00 p.m. - 1.00 a.m., etc.

**207.5 GW (spring), 188.0 GW (summer), 191.5 GW (fall), and 226.2 GW (winter).

4.3. Main Parameters of the Power Plants

The main parameters of the solar power plants are sensitive to the characteristics of the direct solar radiation of the location in question. For instance, with about 60% of potential land considered to be available in Turkey, quite a number of solar plants may be located in that country. In order to choose a realistic parameter for such STEC plants (reliability of electricity supply and of mirror areas as a function of the volume of internal storage), a STECP model run, based on Turkish conditions, was performed for each of the seasons and for the plants with 0.5, 5, 9, 10, and 12 hours of internal storage. The plants were operated in a load following mode (see Table 4). The results of the runs aggregated over the entire year are presented in Table 5.

Note that "losses" are defined as thermal energy losses due to a fully charged storage while the load is being met.

Table 5. Influence of the storage capacity on the load following opportunity of plants II and III.

Storage capacity [hrs]	Losses* (% of production)	Reliability of covering the demands (% of the demands)	Area of the mirrors [km^2]
0	12.4	0.238	0.43
5	11.6	0.47	0.85
9	18.7	0.6692	1.27
10	16.6	0.716	1.38
12	19	0.775	1.62

*Thermal energy losses at fully charged storage during operation.

According to R. Caputo (private communication, IIASA, 1981) this range of "losses" (11.6% - 19%) are acceptable for a plant working in a load-following mode.

The results shown in Table 5 were used to estimate the annual capacity factor and land and mirror areas for the two types of plants, with a 100 MW peak installed capacity, in the respective radiation zones (see Table 6).

Table 6. Summary characteristics of the STEC plants considered.

Plant type	Radi- ation zone	Annual capacity factor	Ground coverage ratio	Area (km^2) Mirrors	Land	Hours of Storage
STEC 1 for peak load	I	0.196	0.3	0.445	1.48	0.5
	II	0.216	0.3	0.437	1.45	0.5
	III	0.23	0.3	0.43	1.43	0.5
STEC 2 for inter- mediate and base loads	I	0.71	0.3	1.8	6.	16
	II	0.71	0.3	1.4	4.7	13
	III	0.716	0.3	1.3	4.6	10

The plants differ above all in terms of the capacity factors adopted. The capacity factor is defined as the share of the year during which a plant is capable of producing electricity at its rated power (i.e., 100 MW). The values adopted for this indicator vary between 0.196 and 0.238 for STEC 1, between 0.71 and 0.716 for STEC 2, depending in both cases on the respective radiation zone.

The levels of 0.2 and 0.7 were chosen to distinguish between plants operable only during sunshine hours (STEC 1) and in a load-following mode (STEC 2). This additional assumption significantly reduces the number of cases that had to be investigated.

The mirror areas and hours of storage required (see Table 6) were determined on the basis of the capacity factors chosen.

4.4. Plant Allocation Strategy

The total land considered available in Table 1 must be juxta-posed to the land requirements of the two types of plants con-sidered. According to Table 6, it is about 1.5 km^2 per plant for STEC 1 and about 5 km^2 for STEC 2. However, there are also plant-specific requirements, for the surface must be either flat or tilted southwards. For lack of detailed information on the availability of such land in the producing countries it has been assumed that no more than 20% of the total potential land may be suitable for solar power plant siting. Consequently, less land was considered suitable for STEC 2 plants than for STEC 1 plants.

If one assumes a total electricity demand of the order of 200 MW (Table 4) and an allocation of 90% STEC 1 and 10% STEC 2 plants with load factors of about 0.2 and 0.7, respectively, about 13,000 plants are needed. Accordingly, two-thirds of the land available is covered by STEC 1 and one-third by STEC 2 plants. This allocation strategy is the base case (Case 3) for comparing the electricity production-demand correlation if a single site (Case 1) or only dispersed STEC 1 plants (Case 2) are used.

Table 7. Allocation of 100 MW plants for Case 3.

Radiation Zone	I		II		III	
Country	STEC 1	STEC 2	STEC 1	STEC 2	STEC 1	STEC 2
Portugal	286	28	0	0	0	0
Spain	1100	108	1263	153	127	16
France	591	58	0	0	0	0
Italy	135	13	315	38	144	18
Yugoslavia	305	30	105	12	0	0
Greece	0	0	158	19	163	21
Turkey	2417	238	2299	278	2386	302
Total (13,126)	4834	475	4140	500	2820	357

4.5. The Cases Considered

Three extreme cases were considered to study the effect of different local climates (radiation) on the overall output of the plants, as well as the influence of internal thermal storage on STEC electricity production.

Case 1. Single site, no thermal storage.

All (13,126) 100 MW units from Table 7 are STEC 1 plants assumed to be concentrated in one place (Carpentras) and operated in a sun-following mode (electricity production during sunshine hours only).

Case 2. Multiple sites, no thermal storage.

STEC 1 plants replace STEC 2 plants listed in Table 7, adding up to the same (13,126) total number of plants (e.g., 314 STEC 1 plants for Portugal). The plants operate in a load-following mode.

Case 3. Multiple sites, with and without thermal storage.

The allocation strategy is to combine STEC 1 and STEC 2 as described in Table 7; the former operate in a sun-following mode and the latter in a load-following mode. Note that about 80% of the plants are located in two of the seven countries (21% in Spain and 60% in Turkey).

5. RESULTS OF THE RUNS

Given these assumptions, the model was run for the three cases and 15 subsequent days per season. Time differences between locations were taken into account. In each case the electrical output was integrated on an hourly basis over the entire period and was compared to the respective electricity demand profile. As a result of this comparison the share of solar electric power plants in satisfying total electrical demands were determined.

It is interesting to compare the above indicator for dispersed STEC 1 plants (Case 2) and dispersed STEC 1 and STEC 2 plants (Case 3) for an average day per season (see Figure 3).

In summer a much higher share of electricity demand can be met in Case 3 than in Case 2. For example, between 5 a.m. and 8 p.m. reliability of supply is as high as 96.7% in Case 3 compared to 40% for Case 2. In spring, fall, and winter, the values for Case 3 are 80%, 70%, and 42%, respectively.

Table 8 gives the solar shares in electricity supply and compares the electricity produced throughout 24 hours for Cases 3 and 2.

The introduction of STEC 2 plants with thermal storage in the system (Case 3) almost doubles the amounts of electricity produced (see Table 8) in summer and increases them up to 3.12 in spring time. Shares of 0.31 to 0.85 of the demand are met in Case 3 but only 0.16 to 0.55 in Case 2. The system's output appears to be very sensitive to the volume of internal storage introduced during the periods of weak and/or highly irregular solar radiation, e.g., fall, winter, and spring. The optimal share of internal storage to be introduced in the system and its dependence on economic indicators could deserve a more detailed study.

Table 8. Influence of thermal storage on solar electricity production.

	Summer		Fall		Winter		Spring	
	Solar share[1]	Ratio[2]	Solar share[1]	Ratio[2]	Solar share[1]	Ratio[2]	Solar share[1]	Ratio[2]
Case 3	0.85		0.552		0.309		0.67	
Case 2	0.55		0.209		0.161		0.21	
Ratio (Case 3/ Case 2)		1.9		2.65		2.98		3.12

[1] Share of electricity demand met by STEC plants;
[2] Ratio of electricity produced in Case 3 to Case 2.
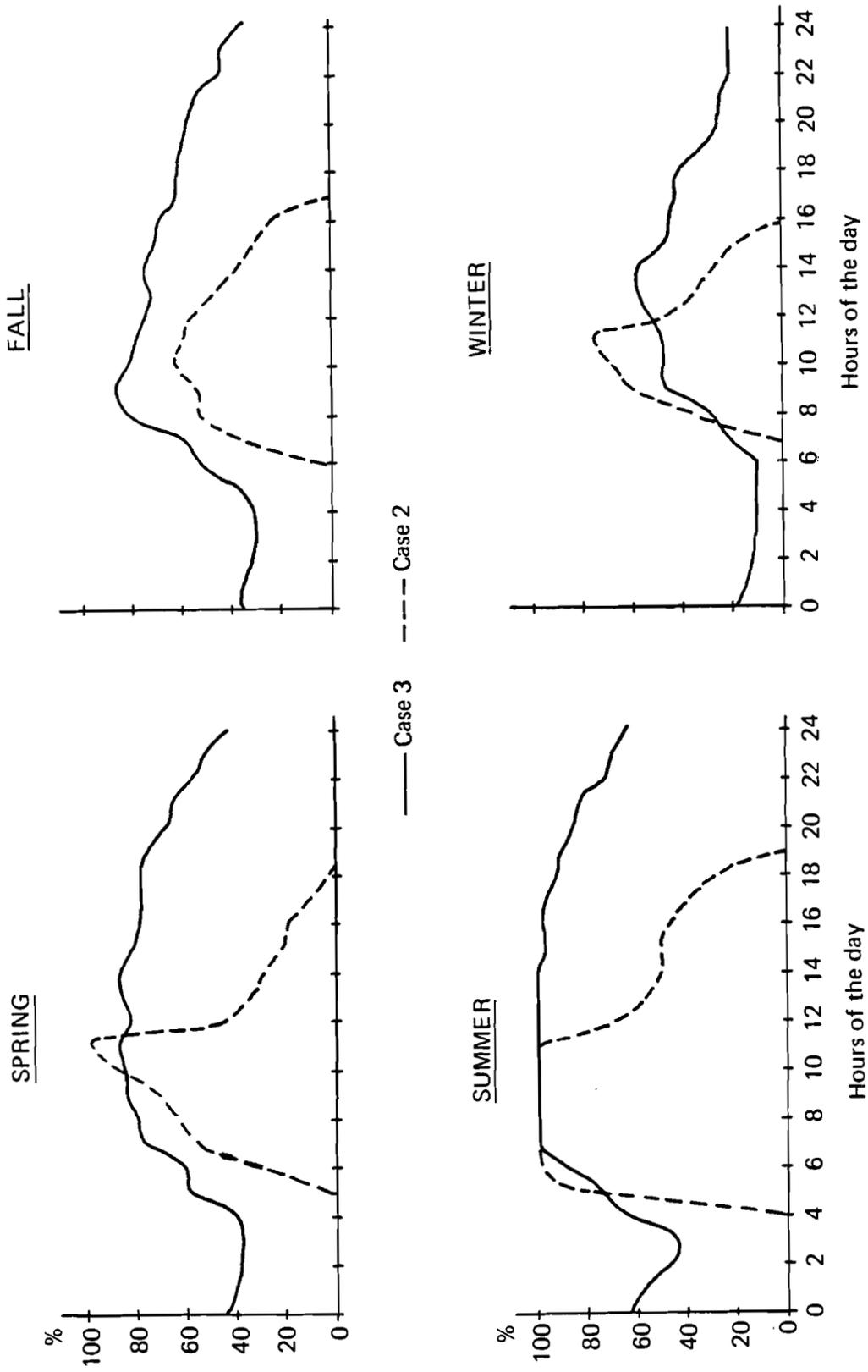
Figure 3. Solar shares in total electricity production.

Comparison of those cases may induce one to look at the electricity production-demand correlation differently: what could be the solar installed capacities and related external daily and seasonal storage requirements if also the rest and thus 100% of the electricity demands should be met by solar-produced electricity?

For exploring that question, an LP-model called ESOM (Electricity and Storage Optimization Model) built by N. Nakicenovic (1982) was used together with the present model. ESOM allows to bridge the gaps between available solar electricity and actual electricity demand by possible introduction of new solar capacities, daily storage, and seasonal storage; the latter is less efficient than daily storage but compensates for seasonal variations in solar radiation levels and electricity demands.

Table 9 gives results of the joint runs of the ESOM and STECP models, comparing Case 1 and Case 2 to Case 3.

Table 9. Comparison of the three case studies; ratios are based on Case 3.

	Yearly solar electricity generation	Solar installed capacities	Daily external storage capacities	Seasonal storage capacity
Case 1	1.071	1.954	1.61	1.51
Case 2	1.048	1.345	1.366	1.
Case 3	1.	1.	1.	1.

Case 1: Single sites, no thermal storage
Case 2: Multiple sites, no thermal storage
Case 3: Multiple sites, thermal storage

Thus it is clear that concentration of the solar plants in one place as in Case 1 requires

-- twice the installed capacities as compared to Case 3, or 1.45 times the installed capacities in the multiple siting Case 2;
-- introduction of 1.6 times more daily storage (1.18 times more than in Case 2);
-- introduction of 50% more of the less effective seasonal storage than in the other two cases.

Through a dispersed siting of the solar plants, even without introduction of internal storage (Case 2 against Case 1) only 69% solar capacities, 85% daily storage, and 66% seasonal storage are needed.

A second, broader comparison between Cases 3 and 2 shows that an introduction of 10% STEC plants with an internal storage in the system (Case 3) reduces both the solar installed capacities and the daily external storage capacities by about 35%.

Some further parametric studies, taking into account the systems limitations for introduction of external storage, grid losses, and some site-specific cost indicators for both internal and external storage, could lead to more precise results.

CONCLUSION

STECP, a model simulating solar thermal electricity conversion performance, has been described and used to study the electricity supply-demand correlation for a system of dispersed solar electric plants supplying electricity to a large number of European countries. This effort has led to several concrete results.

-- The results of the study can be used to evaluate the performance parameters of a system of solar plants in order to include them in an energy supply model.
-- The hourly solar shares in total electricity produced over the season were evaluated.
-- On the basis of those shares for each season, an investigation was made of the amounts of external storage to be included in the system, in order to meet 100% of the electricity demand by solar plants.
-- It appears that spreading the locations of solar plants increases the reliability of meeting the demand.
-- Introduction of internal thermal storage in a system of dispersed solar plants increases their seasonal output from two to three times while decreasing the external storage requirements.

REFERENCES

Balabanov, T. 1981. Solar Tower in Bulgaria. Doctoral thesis.
    Sofia: Technical University.

Budyko, M.I. 1963. Atlas of the Heat Balance of the Earth.
    B-26 (in Russian). Leningrad, USSR: Kartfabrika Gosgeol-
    techizdata.

Duffie, J. 1974. Solar Energy Thermal Processes. New York:
    J. Wiley & Sons.

EEC. 1979. Atlas of Solar Radiation in Europe. Vol. 1.
    Global Radiation on a Horizontal Surface (in German).
    Dortmund, F.R.G.: W. Grösschen-Verlag.

French Meteorological Service. 1980. Fichier Climatologiques
    de Trappes et de Carpentras. Paris: Ministère des Trans-
    ports, Direction de la Météorologie.

Fujita, T. et al. 1978. Solar Thermal Systems Performance
    Algorithms. Pasadena, California: Jet Propulsion Labora-
    tory.

Liu, B.Y.H., and R.C. Jordan. 1960. The Interrelationship and
    Characteristic Distribution of Direct, Diffuse and Total
    Solar Energy 4(3):1-12. Oxford: Pergamon Press.

Löf, G.O.G., J.A. Duffie and C.O. Smith. 1966. World Distri-
    bution of Solar Radiation. Report No. 21. Engineering
    Experimental Station. Madison, Wisconsin: The University
    of Wisconsin.

Nakicenovic, N. 1982. Electricity and Storage Optimization Model. Laxenburg, Austria: International Institute for Applied Systems Analysis. Forthcoming.

Riaz, M. 1976. A Theory of Concentrations of Solar Energy on a Central Receiver to an Electric Power Generation. Journal of Engineering for Power, 373-383.

Union pour la Coordination de la Production et du Transport de l'Electricité (UCPTE). 1979. 151, Boulevard Haussmann, F-75008 Paris.

USSR Hydrometeorological Service. 1976. Solar Radiation and Radiation Balance Network, Annual Data. 1969-1973, Part 2. USSR: Leningrad.

Ward, T. 1982. Estimation of the Long Term Potential of Soft Solar Energy in the Housing Sector of Western Europe. Laxenburg, Austria: International Institute for Applied Systems Analysis. Forthcoming.